ISBN: 978-3-95450-204-2 ISSN: 2673-5350 doi:10.18429/JACoW-IBIC2019-WEPP039

SINGLE-SHOT DIAGNOSTICS OF MICROBUNCHED ELECTRONS IN LASER-DRIVEN PLASMA ACCELERATORS AND FREE-ELECTRON LASERS*

Alex H. Lumpkin†, Fermi National Accelerator Laboratory, Batavia, IL 60510 USA
Donald W. Rule, Silver Spring MD, 20904 USA

Abstract

In general, the inherent statistical variances in the laser-driven plasma accelerators (LPAs) and self-amplified spontaneous emission (SASE) free electron lasers (FELs) motivate the use of single-shot diagnostics. In addition, the microbunching phenomenon in each is also variable, so coherent optical transition radiation (COTR) techniques also warrant single-shot evaluations. In both cases, the enhancements of the signals enable optical beam splitters to be used to direct light to the different measuring devices for electron beam size, divergence, spectral content, and/or bunch length as appropriate. COTR Interferometry (COTRI) modelling results for the pre-buncher case at 266 nm and for the LPA case at 633 nm are presented. In addition, examples of few-micron beam size and sub-mrad beam divergence measurements from a single shot of an LPA are reported.

INTRODUCTION

The need for single-shot diagnostics of the periodic longitudinal density modulation of relativistic electrons at the resonant wavelength (microbunching) in a free-electron laser (FEL) or at broadband visible wavelengths as in a laser-driven plasma accelerator (LPA) has been reaffirmed. In the self-amplified spontaneous emission (SASE) FEL case, statistical fluctuations in the microbunching occur in the start-up-from-noise process. In the LPA, the plasma itself is chaotic and varies shot to shot. Fortunately, we have shown that coherent optical transition radiation (COTR) techniques, can assess beam size, divergence, spectral evolution, and z-dependent gain (10^5) of microbunched electrons in a past SASE FEL experiment at 530 nm [1]. We consider a potential use of such diagnostics for the microbunched electrons following a pre-buncher involving a seed laser, modulator, and chicane for 266 nm. Recently, the application of COTR-based diagnostics to LPAs has been demonstrated with single-shot near-field (NF) and far-field (FF) COTR imaging done at the exit of an LPA for the first time [2,3]. Both configurations will be described with modelling of COTRI for the first and second cases with examples of data for the second.

* This manuscript has been authored by Fermi Research Alliance, LLC under Contract No. DE-AC02-07CH11359 with the U.S. Department of Energy, Office of Science, Office of High Energy Physics.
† lumpkin@fnal.gov

EXPERIMENTAL ASPECTS

The APS Linac

The APS linac is based on an S-band thermionic cathode (TC) rf gun which injects beam into an S-band linear accelerator with acceleration capability currently up to 450 MeV. This is an S-band pulse train with about 10 ns macropulse duration and 28 micropulses, presently delivering 1 to 1.5 nC per macropulse. Beam diagnostics in the linac include imaging screens, rf BPMs, loss monitors, and coherent transition radiation (CTR) autocorrelators.

For possible experiments for imaging microbunched electrons due to a pre-buncher, the beam is transported to the Linac Experimental Area (LEA) tunnel [4] where the pre-buncher is staged as schematically shown in Fig. 1. In the considered case, a 266-nm wavelength seed laser is co-propagated with the 375-MeV electron beam through a modulator to energy modulate the beam. A small chicane magnet array is used to provide the R_{56} term for converting this to the longitudinal modulation, or microbunching at 266 nm. An insertable foil is used to block the seed laser for the COTR measurements. A NF image of the beam size is obtained from forward COTR emitted from the back surface. In addition, a mirror rotated at 45° to the beam direction and located 6.3 cm downstream redirects the light to the optics. This same mirror is the source for backward COTR that interferes with the COTR from the first source to form interference patterns in the angular distribution patterns recorded in the FF camera.

Due to the enhancements of the COTR, the signal may be split among the five measurement options as indicated in Fig. 2. For this case the NF image, FF image, spectral content, COTR gain, and bunch length could be assessed on a single shot. Even with the sampling entrance slits of the spectrometer and streak camera, the signals should be strong enough for statistically relevant data.

Laser-driven Plasma Accelerator Aspects

For the LPA, the basic arrangement is shown in Fig. 3 with the 150 TW laser of central wavelength 800 nm, gas jet, the foil wheel, and the downstream mirror at 45° to the beam direction. A similar two source geometry is used as in the pre-buncher scenario, only L=18.5 mm in this case, and the beam energy is about 215 MeV [3]. In the experiment the FF image is filtered with a 633 ± 5 nm bandpass filter (BPF) which is narrow enough so that the fringe visibility is dependent on only the beam divergence.

ISBN: 978-3-95450-204-2 ISSN: 2673-5350 doi:10.18429/JACoW-IBIC2019-WEPP039

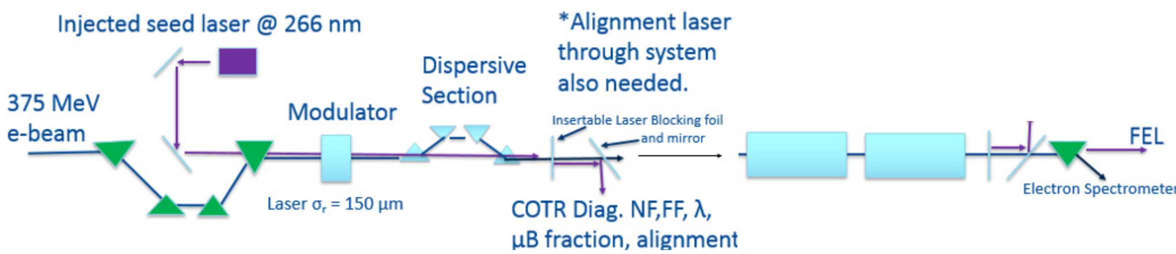

Figure 1: Schematic of the injection seed laser, modulator, dispersive section, COTRI diagnostics, some of SASE FEL undulators, and electron spectrometer at the end of the LEA beamline.

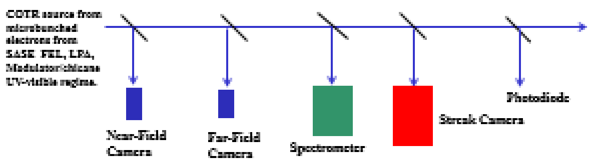

Figure 2: Schematic of single-shot COTR diagnostics for beam size, divergence, spectrum, bunch length, and energy.

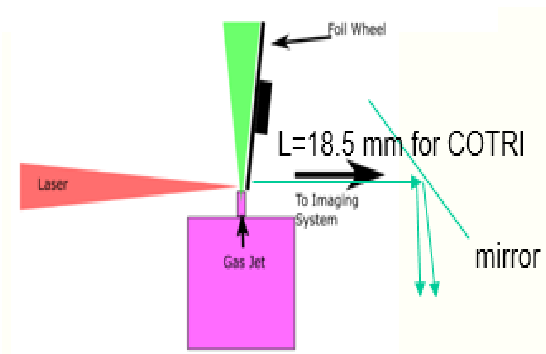

Figure 3: Schematic of LPA with 150 TW laser, He gas jet, Laser blocking foil wheel, mirror, and COTR source separation of 18.5 mm [3].

ANALYTICAL MODEL AND RESULTS

Optical Transition Radiation Basics

When a charged-particle beam transits the interface of two different media, optical transition radiation (OTR) is generated by induced currents at the boundary of those media with different dielectric constants. There are forward and backward radiation cones emitted with opening angle of 1/γ (where γ is the relativistic Lorentz factor) around the angle of specular reflection for the backward OTR and around the beam direction for the forward OTR. For a nominal case of 375 MeV, a foil separation L= 6.3 cm, a wavelength of 266 nm, and a beam divergence of 0.1 mrad, one obtains the two-foil angular distribution pattern (red curve) as shown in Fig. 4, which is compared to the single foil pattern (black curve). The fringe visibility decreases with larger divergence values, and this dependence then can be used for a divergence measurement.

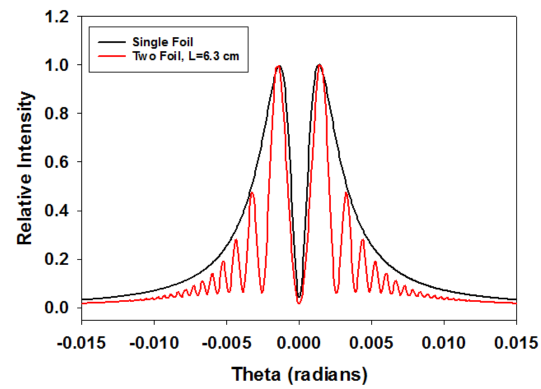

Figure 4: Comparison of far field OTR angular distribution patterns for a single foil (black curve) and a two-foil interferometer (red curve). A beam energy of 375 MeV, wavelength of 266 nm, L=6.3 cm, and a divergence of $\sigma_\theta = 0.1$ mrad were used in the calculations.

The number W_1 of OTR photons that a single electron generates per unit frequency ω per unit solid angle Ω is

$$\frac{d^2W_1}{d\omega d\Omega} = \frac{e^2}{\hbar c}\frac{1}{\pi^2\omega}\frac{(\theta_x^2+\theta_y^2)}{(\gamma^{-2}+\theta_x^2+\theta_y^2)^2} \qquad (1)$$

where $\hbar$ is Planck's constant/2π, e is the electron charge, c is the speed of light, and θ_x and θ_y are radiation angles [5].

COTRI Model Results at 266 nm

The addition of the interference term $I(\boldsymbol{k})$ and the coherence function $J(\boldsymbol{k})$ as shown in Eqs. 2-5 include the effects of the microbunched fraction $f_B=N_B/N$, N_B being the microbunched part of the total N.

$$\frac{d^2W}{d\omega d\Omega} = \left|r_{\parallel,\perp}\right|^2 \frac{d^2W_1}{d\omega d\Omega}\,\boldsymbol{I}(\boldsymbol{k})\boldsymbol{J}(\boldsymbol{k}) \qquad (2)$$

$$\boldsymbol{I}(\boldsymbol{k}) = 4\sin^2[\tfrac{kL}{4}(\gamma^{-2}+\theta_x^2+\theta_y^2)] \qquad (3)$$

$$\boldsymbol{J}(\boldsymbol{k}) = N + N_B(N_B-1)|H(\boldsymbol{k})|^2 \qquad (4)$$

$$H(\boldsymbol{k}) = \frac{\rho(\boldsymbol{k})}{Q} = g_x(k_x)\,g_y(k_y)\,F_z(k_z) \qquad (5)$$

where $H(\boldsymbol{k})$ is the Fourier transform of the charge form factors for a single microbunch [5].

The COTRI calculations with the same parameters as Fig. 4 except with $N_B > 0$, for 25, 50 and 100 µm beam sizes show the effect of the microbunched transverse size

ISBN: 978-3-95450-204-2 ISSN: 2673-5350 doi:10.18429/JACoW-IBIC2019-WEPP039

on the coherence function as a function of angle in Fig 5a. The smallest beams result in the largest angles over which fringes are enhanced. The maximum enhancement is on axis at zero radians in Fig.5b and shows a gain of $7x10^6$ for this case of $f_B = 0.10$ microbunching fraction with 300 pC micropulse charge. A noticeable loss of the outer fringe enhancements for these larger beam sizes is observed in Fig. 5a when compared to Fig. 4.

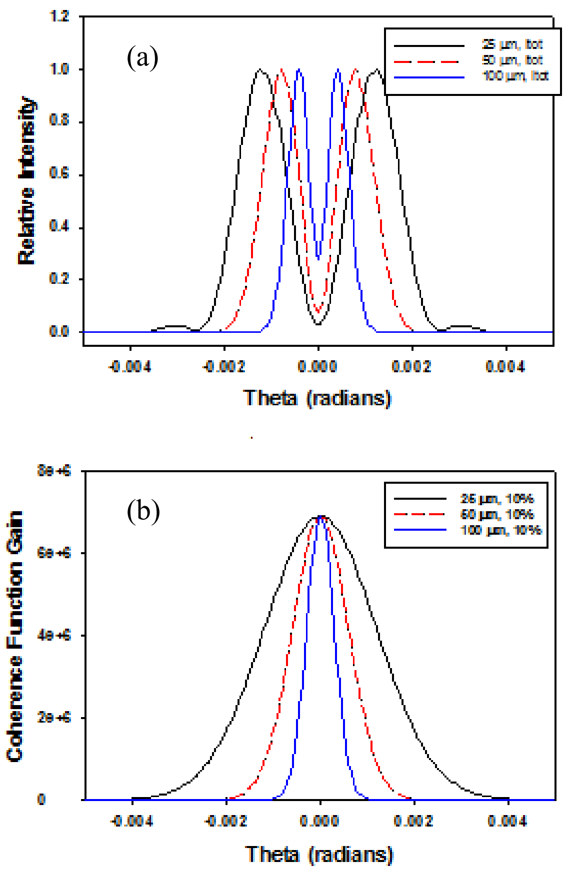

Figure 5: COTRI calculations for (a) interference fringes for L= 6.3 cm and (b) the coherence function for beam sizes of 25, 50, and 100 µm. The outer fringes seen in Fig. 4 have not been enhanced for these larger beam sizes.

COTRI Model Results at 633 nm

As another example, we consider the interferometry case for the LPA at 215 MeV where L=18.5 mm and λ=633 ± 5 nm as shown in Fig. 6. With the beam size of 2 µm, the coherence enhancement extends to -20 mad for the negative angles. The divergence effects for the 0.5 and 1.0 mrad cases show the fringe visibility is better for the lower divergence. For the positive angles, we show the effects of microbunched beam size on the coherence function. At 10 and 20 µm the outer fringes are much less enhanced compared to the 4-µm case. The number of fringes observed gives a coarse measure of the beam size.

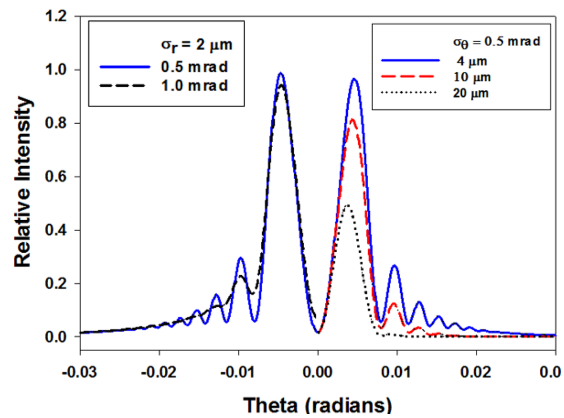

Figure 6: COTRI calculations for the LPA case with L=18.5 nm and λ=633 ± 5 nm showing the divergence effect for fixed 2 um beam size for negative angles and the beam-size effect for positive angles for fixed beam divergence of 0.5 mrad [6].

LPA COTR EXPERIMENTAL RESULTS

For the LPA case for single-shot diagnostics, we consider the NF and FF images shown in Fig. 7 obtained from the COTR foils located 2 mm and 18.5 mm after the LPA exit. The vertically polarized NF image is dominated by the point spread function, and analysis leads to a beam size of 2.6 µm for each of the two beamlets that are about 6 µm apart horizontally, which is the laser polarization axis direction. The FF COTRI image fringe visibility was compared to the patterns in Fig. 6 and additional model results to obtain the divergence estimate of 0.5 ± 0.2 mrad. The divergence of the microbunched portion of the beam is less than that of the ensemble of electrons measured at the downstream spectrometer screen. The normalized emittance estimate from the product of these two values from the subset of electrons is ~0.5 mm mrad at 215 MeV.

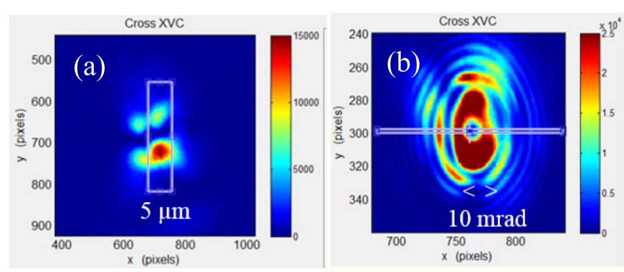

Figure 7: Examples of single-shot imaging for the LPA case (a) NF image with PSF dominated structure (b) FF image showing interference fringes in the angular distribution pattern with L=18.5 mm and λ=633 ±5 nm [6].

SUMMARY

In summary, we have presented model results for a pre-buncher for a SASE FEL, model results for the LPA, and examples of NF and FF COTR images from the LPA microbunching case. The TW laser, seed laser, or FEL light can be blocked by a first, thin foil to enable the COTR sources to be cleanly detected and analysed. Due to the high COTR/OTR gain the signal can be split to several detectors to provide single-shot diagnostics of the beam.

ISBN: 978-3-95450-204-2 ISSN: 2673-5350 doi:10.18429/JACoW-IBIC2019-WEPP039

ACKNOWLEDGMENTS

The first author acknowledges the support of C. Drennan and M. Lindgren at Fermilab. The authors acknowledge M. LaBerge and Prof. M. Downer of the University of Texas at Austin for the experimental realization of the single-shot COTR diagnostic images shown in Fig. 7.

REFERENCES

[1] A. H. Lumpkin *et al.*, "Evidence for Microbunching Sidebands in a Saturated Free-electron Laser Using Coherent Optical Transition Radiation", Phys. Rev. Lett. **88**, No.23, 234801, 2002.

[2] M. LaBerge *et al.*, talk presented at EAAC17, Elba, Italy, Sept. 2017.

[3] A.H. Lumpkin, M. LaBerge, D.W. Rule *et al.*, "Observations of COTR Interference Fringes Generated by LPA Electron Beamlets", Proc. of AAC18, Breckenridge, CO (IEEE) (2019).

[4] Y. Sun *et al.*, "APS LINAC Interleaving Operation", in *Proc. 10th Int. Particle Accelerator Conf. (IPAC'19)*, Melbourne, Australia, May 2019, pp. 1161-1163. doi:10.18429/JACoW-IPAC2019-MOPTS119

[5] D. W. Rule and A. H. Lumpkin, "Analysis of Coherent Optical Transition Radiation Interference Patterns Produced by SASE-Induced Microbunches", in *Proc. 19th Particle Accelerator Conf. (PAC'01)*, Chicago, IL, USA, Jun. 2001, paper TPAH029, pp. 1288-1290.

[6] A.H. Lumpkin, M. LaBerge, D.W. Rule, et al., "Interferometric Optical Signature of Electron Microbunches from Laser-Driven Plasma Accelerators", submitted to Phys. Rev., http://arxiv.org/abs/1907.05078